Influence of MnO_2 decorated Fe nano cauliflowers on microwave absorption and impedance matching of polyvinylbutyral (PVB) matrix

2016 Mater. Res. Express 3 095003

IOP Publishing Mater. Res. Express 3 (2016) 095003 doi:10.1088/2053-1591/3/9/095003

Materials Research Express

CrossMark

RECEIVED
3 August 2016

REVISED
13 August 2016

ACCEPTED FOR PUBLICATION
18 August 2016

PUBLISHED
2 September 2016

PAPER

Influence of MnO_2 decorated Fe nano cauliflowers on microwave absorption and impedance matching of polyvinylbutyral (PVB) matrix

Pritom J Bora[1], Mayuri Porwal[2], K J Vinoy[3], Praveen C Ramamurthy[1,2] and Giridhar Madras[1,4]

[1] Interdisciplinary Centre for Energy Research (ICER)
[2] Department of Materials Engineering
[3] Department of Electrical and Communication Engineering
[4] Department of Chemical Engineering, Indian Institute of Science, Bangalore-560012, India

E-mail: onegroupb203@gmail.com

Keywords: Fe nano cauliflower, MnO_2 nanofiber, PVB composite, microwave absorption, EM attenuation constant

Abstract

In this work, a promising, polyvinyl butryl (PVB)-MnO_2 decorated Fe composite was synthesised and microwave absorption properties were studied for the most important frequency ranges i.e., X-band (8.2–12.4 GHz) and Ku-band (12.4–18 GHz). The microwave absorption of Fe nano cauliflower structure can be enhanced by MnO_2 nanofiber coating. 10 wt% Fe–MnO_2 nano cauliflower loaded PVB composite films (2 mm thick) shows an appreciable increase in microwave absorption properties. In X-band, the reflection loss (RL) of this composite decreases almost linearly to −7.5 dB, whereas in the Ku-band the minimum RL was found to be −15.7 dB at 14.7 GHz. Here it was observed that impedance matching is the primarily important factor responsible for enhanced microwave absorption. Further, enhancement of EM attenuation constant (α), dielectrics, scattering attenuation also bolsters the obtained results. This polymer composite can be considered as a novel microwave absorbing coating material.

1. Introduction

The proliferation of communication systems, digital systems, miniaturisation of electronic devices and components and the development of superfast processors have led to the emergence of electromagnetic compatibility [1]. The microwave absorbers, especially core–shell structures, are becoming increasingly important for the radio, high frequency devices, local area network devices, as well as special applications like military and stealth technology [2]. Phase matching and impedance matching are two important phenomena involved in microwave absorption. However, impedance matching plays a key role for microwave absorption from the materials point of view [3]. The reflection loss (RL) takes place in the material by various mechanisms like dielectric loss, conduction loss (electric loss) as well as hysteresis and domain wall resonance (magnetic loss) [4]. Inevitably, composite materials having combinations of dielectric and magnetic materials, such as nanocomposites, provide the desired combination of low reflection and high loss [1, 5].

In the recent times, polymer nanocomposites are increasingly being used for electromagnetic interference shielding and microwave absorption [5]. Polymer nanocomposites incorporating appropriate filler material provide a unique balance of physical and mechanical properties like lightweight, low density, ease of processability and corrosion resistance [6]. Incorporating magnetic particles in a composite increases its microwave absorption ability due to the improved complex permeability [7]. Iron (Fe) and its oxides (Fe_2O_3) is one of the most common and promising metallic ferromagnetic material to be incorporated in composites for microwave absorption because of its excellent properties like high Snoek's limit and permeability, high Curie temperature as well as high saturation magnetisation [8]. Guo *et al* [9] studied the self-assembled flower like iron oxide nanoparticles for microwave absorption. For 80 wt% γ-Fe_2O_3 flower/epoxy composites of thickness

3 mm, they reported a RL of −15 dB at 3.4 GHz [9]. Wu *et al* studied the microwave absorption of Fe fibre-epoxy resin composites [10]. According to their study, optimum −11 dB RL can be reached by loading 20 wt% Fe fibre to epoxy resin at 7.5 GHz for the thickness of 1.5 mm [10]. Moreover, their study shows the thickness dependency of microwave absorption of low permeability materials. Wang *et al* studied the microwave absorption properties of γ-Fe_2O_3, Fe_3O_4 and Fe nanoparticles in ordered mesoporous carbons [7]. They reported −32 dB RL in the range of 11–12 GHz for 40 wt% loaded Fe_3O_4-CMK-3 and γ-Fe_2O_3-CMK-3 to epoxy matrix (thickness 1.6 mm) [7].

Among the various metal oxides that can be used in polymer nanocomposites for microwave absorption, MnO_2 has received a lot of attention due to its dielectric and other unique properties. Song *et al* reported that 30 wt% β-MnO_2 nanorod loaded paraffin wax composite shows a RL of −10 dB (∼11 GHz) at 2.75 mm thickness [11]. Duan *et al* studied β-MnO_2 micron cube with rectangular pyramid/paraffin composites and reported a RL of −13 dB at 15.5 GHz (thickness 2 mm) [12]. In a related work, they reported that the low temperature annealed α-MnO_2 has better microwave absorption with frequency. They reported ∼−13.5 dB RL value at 18 GHz for 30 wt% MnO_2 loaded paraffin nanocomposite (thickness 2 mm) [13]. Lv *et al* studied the microwave absorption of graphene-MnO_2 nanorod-Fe nanocomposites. According to their result, graphene–MnO_2–Fe loaded paraffin wax (1:1) displays −15 dB RL at 12 GHz for a thickness of 3 mm [3].

Polyvinylbutyral (PVB) has recently become one of the most attractive polymers due to its dielectric, moisture resistance, good mechanical properties as well as good adhesion to particles [14–16]. Hence, it can be expected that a composite incorporating Fe and MnO_2 nanoparticles in the PVB matrix can exhibit good microwave absorption properties. The objective of the present work was to synthesise and examine the microwave absorption property of PVB–MnO_2 decorated Fe composite.

2. Experimental

2.1. Synthesis of MnO_2 decorated Fe nanoparticles

In the first step, Fe nanoparticles were synthesised by standard heterogeneous precipitation and thermal reduction method [17]. In this synthesis scheme, 100 ml of 0.5 M $FeSO_4$ was prepared and to this solution 1 M NH_4HCO_3 was added at a rate of 3 ml min^{-1} under stirring. The pH of the solution was adjusted to 7–8 by adding few drops of 1 M NaOH. The solution was kept for stirring another 3 h under same conditions. The obtained precipitate was filtered and washed with distilled (DI) water several times and kept in vacuum oven at 80 °C for 12 h. Further it was reduced under nitrogen at 600 °C for 2 h.

In the second step, 0.3 g of PEG (8000) was dissolved in 100 ml DI water and the as synthesised Fe nanoparticles (1.5 g) were dispersed. To this solution, 20 ml of 0.05 M $KMnO_4$ solution was added. After 15 min, 3 ml of 5 M HCl was added very slowly and the solution was allowed to stir for another 2 h. After that, the obtained precipitates was filtered and several times washed with DI water. Finally, it was vacuum dried at 120 °C for 12 h.

2.2. Preparation of PVB–Fe–MnO_2 nanocomposites

The PVB–Fe–MnO_2 nanocomposites were prepared by solution processing. For a stock solution preparation, 3 g of commercially available PVB was dissolved in 10 ml ethanol. To this solution 10 wt% of as synthesised Fe–MnO_2 was added and kept stirring for another 1 h. After that 5 ml DI water was drop wise added to this solution and the hydrophobic gel was washed several times with DI water and poured into rectangular silver moulds (sample holder used for microwave absorption study) and kept for open air drying (48 h). Similarly, for a comparison PVB–Fe composite was also prepared. The prepared PVB–Fe–MnO_2 and PVB–Fe composites were indexed as PVBMF and PVBF, respectively.

3. Characterisations

The prepared samples were coated over carbon tape and sputter coated with gold to examine the surface morphology by using high-resolution scanning electron microscope (SEM, Carl Zeiss). The complex *S*-parameters measurement was carried out by using a vector network analyser (VNA, Agilent NS230A). The complete two-port calibration of the VNA (thru-reflect-line or TRL standard) was performed in the X-band (8.2–12.4 GHz) and Ku-band (12.4–18 GHz) before taking the measurements. From the obtained *S*-parameters ($S_{21}, S_{12}, S_{11}, S_{22}$), the complex permittivity ($\varepsilon^* = \varepsilon' - \mathrm{i}\varepsilon''$) and permeability ($\mu^* = \mu' - \mathrm{i}\mu''$) values were calculated by using standard Nicolson–Ross–Weir algorithm [18]. The prepared PVBF and PVBMF composites were Cu backed for RL measurement (S_{11}). As the composites were Cu backed, the impedance matching ($Z_{\mathrm{in}}/Z_{\mathrm{o}}$) is obtained from the following relation [19], Impedance matching $(Z_{\mathrm{in}}/Z_{\mathrm{o}}) = (1 + S_{11})(1 - S_{11})$.

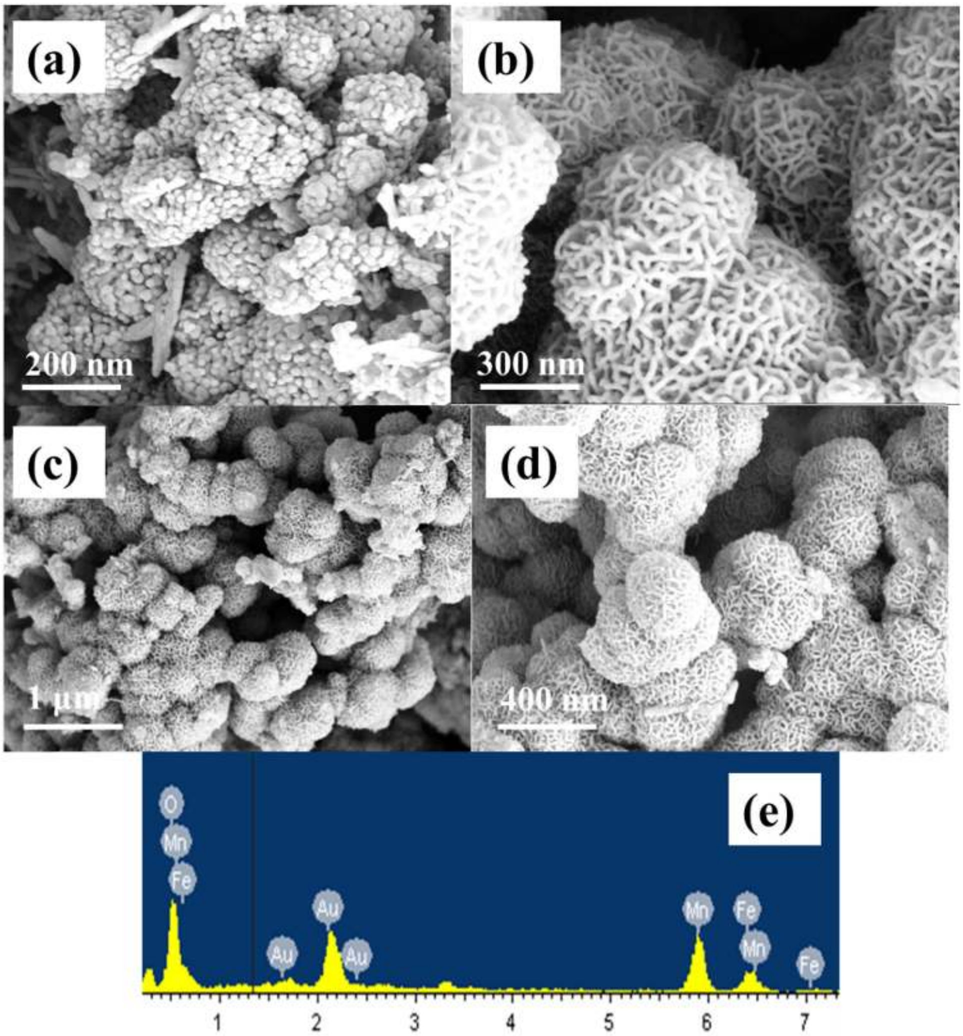

Figure 1. Surface morphology of the as synthesised (a) Fe, (b)–(d) MnO_2–Fe and (e) EDX of MnO_2–Fe composite.

4. Results and discussion

The surface morphology of the as synthesised Fe, MnO_2 decorated Fe nanoparticles were shown in the figure 1. As shown in figure 1(a), the observed surface morphology of the synthesised Fe shows that the Fe nanoparticles form a group of clusters of size 350–400 nm which is similar to cauliflower shape. Figures 1(b)–(d) shows the surface morphology of synthesised Fe–MnO_2 nanocomposite, the MnO_2 nanofibers covered Fe fully and size was observed to be ~500–550 nm. The obtained surface morphology suggests the improvement of loss factor as dielectric loss can takes place along the MnO_2 nanofibers (due to the polarisation in between the interfaces of core–shell) and antenna mechanism of microwave absorption is also applicable for this surface morphology [20].

According to antenna mechanism of microwave absorption, MnO_2 nanofibers can act as a receiving antenna for incident electromagnetic energy which transforms it to dissipative current [20]. Further, the multi interfaces between antenna frame, presence of polymer matrix and air gap can enhance the microwave absorption property [20]. EDX confirms the presence of Fe and Mn (figure 1(e)). The cross sectional SEM image of the prepared PVBMF composite is shown in the figures 2(a) and (b). To investigate the distribution of MnO_2–Fe nano cauliflowers in PVB matrix, elemental mapping was carried out. Figures 2(d) and (e) shows the elemental mapping of Fe and Mn respectively in the PVBMF composite. The homogeneous elemental mapping of Fe and Mn was observed and it suggests the uniform distribution of MnO_2 decorated Fe in PVB matrix.

The variation of real (ε') and imaginary part (ε'') of complex permittivity ($\varepsilon^* = \varepsilon' - i\varepsilon''$) of as prepared PVBF and PVBMF composites in X-band (8.2–12.4 GHz) and Ku-band (12.4–18 GHz) frequency is shown in the figures 3(a), (b) and 4(a), (b) respectively. The real part (ε') of the complex permittivity ($\varepsilon^* = \varepsilon' - i\varepsilon''$) is associated with amount of polarisation which corresponds to the storage ability of the electric energy and

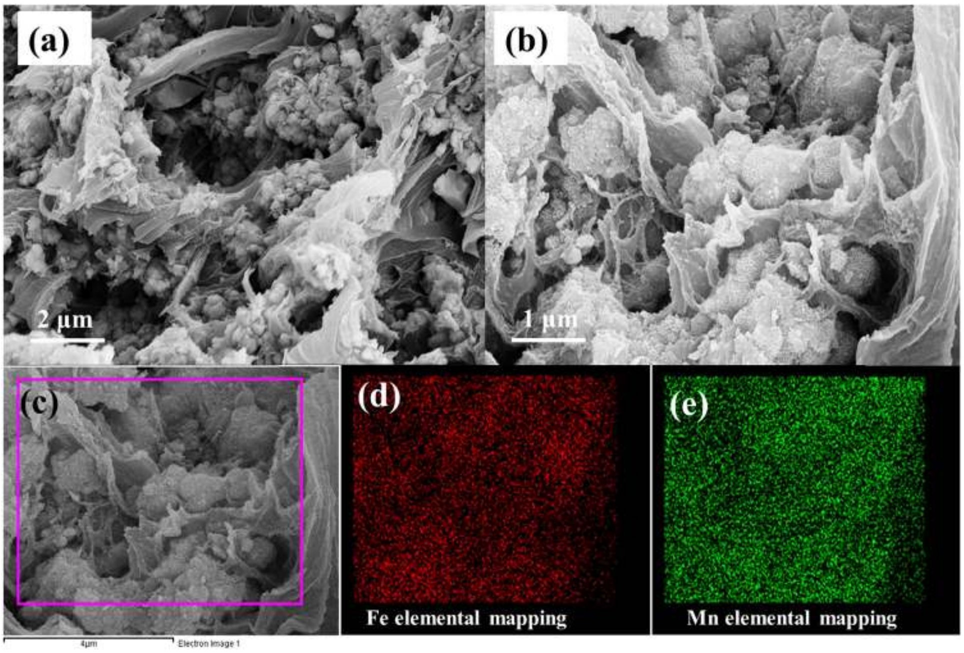

Figure 2. Cross sectional SEM images of (a)–(c) PVBMF composite, (d) elemental mapping of Fe and (e) elemental mapping of Mn in PVBMF composite.

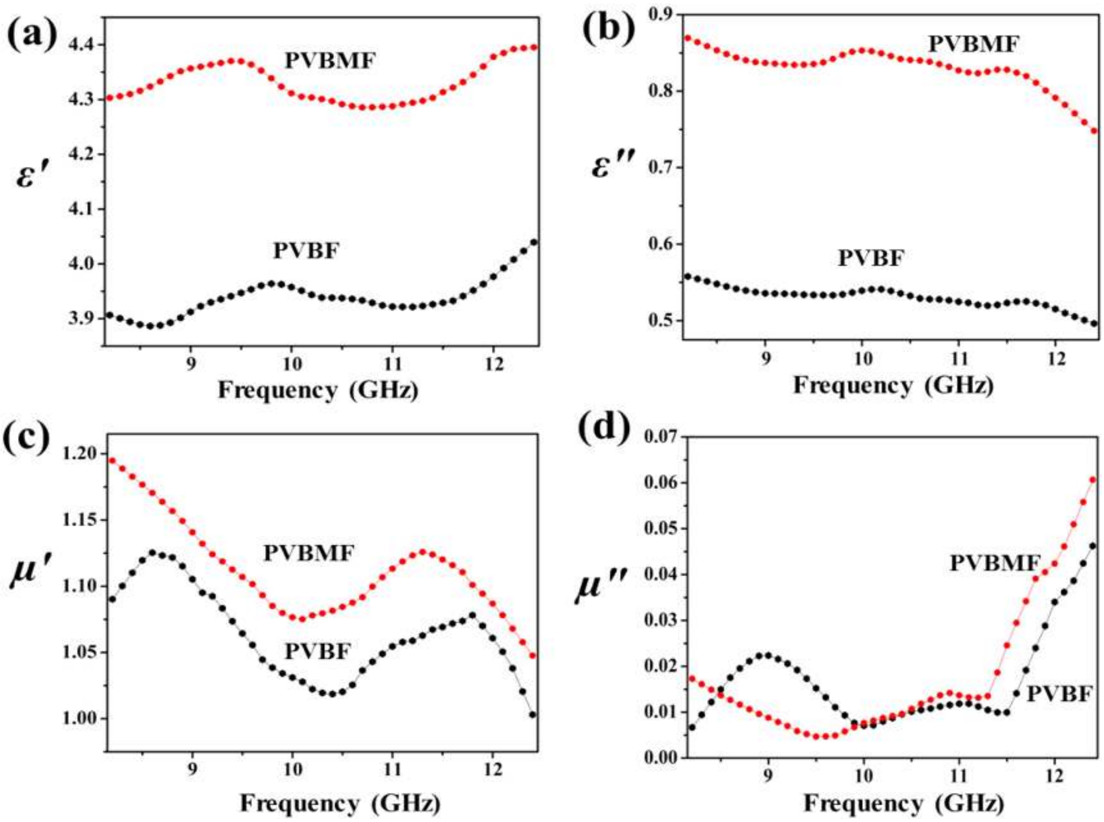

Figure 3. Variation of (a) real part (ε') and (b) imaginary part (ε'') of complex permittivity ($\varepsilon^* = \varepsilon' - i\varepsilon''$) and (c) real part ($\mu'$) and (d) imaginary part (μ'') of complex permeability ($\mu^* = \mu' - i\mu''$) of PVBMF and PVBF composite in the X-band (8.2–12.4 GHz).

imaginary part (ε'') associated with dissipation of electric energy. In the X band, the ε' was found 3.9–4 for PVBF composite, whilst ε'' was between 0.55–0.5. The ε' and ε'' increases to 4.3–4.4 and 0.8–0.7 respectively when 10 wt% of MnO_2 coated Fe (nano cauliflower) was loaded to PVB (PVBMF). No significant change in the ε' and

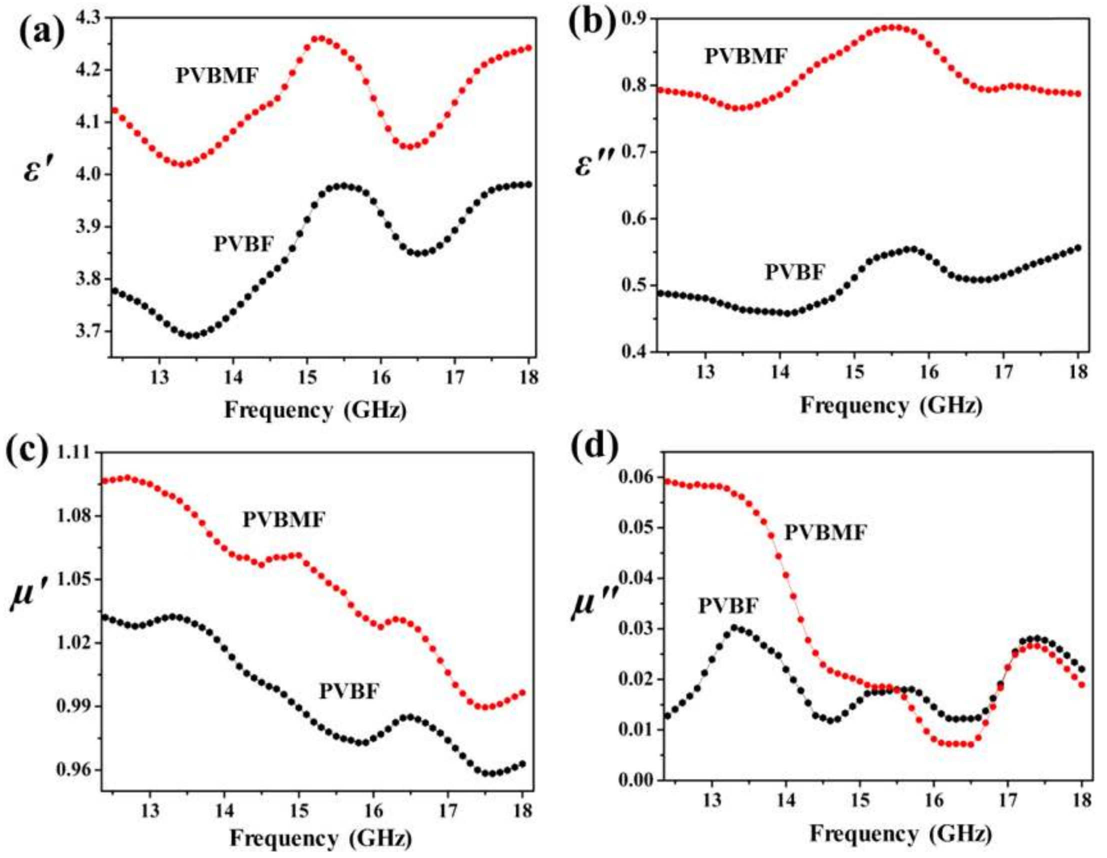

Figure 4. Variation of (a) real part (ε') and (b) imaginary part (ε'') of complex permittivity ($\varepsilon^* = \varepsilon' - i\varepsilon''$) and (c) real part ($\mu'$) and (d) imaginary part (μ'') of complex permeability ($\mu^* = \mu' - i\mu''$) of PVBMF and PVBF composite in the Ku-band (12.4–18 GHz).

ε'' values was observed for PVBMF composite in Ku band (figures 4(a) and (b)). However, a noticeable variation was observed in between 15 and 16 GHz. Figures 3(c) and (d) shows the variation of real (μ', corresponds to storage ability of magnetic energy) and imaginary part (μ'', corresponds to dissipation of magnetic energy) of complex permeability ($\mu^* = \mu' - i\mu''$) of the PVBF and PVBMF composite in the X and Ku-band respectively. Compared to μ', μ'' is negligible for both the composites (figures 4(c) and (d)).

The presence of MnO_2 coated Fe in PVB matrix increases the heterogeneity of the composite system and the oriental polarisation also increases. This could be another reason for the observed dielectric behaviour. Furthermore, the change of the applied electromagnetic field is faster than that of the induced current over MnO_2–Fe nano cauliflowers in the PVB matrix.

The prepared PVBF and PVBMF composite was Cu backed for microwave absorption study in the X-band and Ku-band. The importance of introducing a perfect conductor (Cu) at the back of the composites is that it behaves as a load of transmission line and completes transmission line model [21]. The variation of obtained RL of PVBF and PVBMF composites in the X-band and Ku-band were shown in the figures 5(a) and (b), respectively. In the X-band, as shown in figure 5(a), the RL value of 2.5 mm thicker PVBF composite decreased linearly from −2 dB to −4 dB. On the other hand, for PVBMF composite, it decreased to −8 dB at a thickness of ~2 mm. Similarly, in the Ku-band (figure 5(b)), the RL value of PVBMF composite decreased from −7.5 dB to the minimum −15.7 dB at 14.7 GHz, whereas the PVBF composite shows minimum RL value −9.6 dB at same frequency. Thus, it suggests that, the presence of MnO_2 coated Fe enhances microwave absorption in PVB. A tabulation of RL of as prepared PVBMF composite with various reported materials is shown in table 1. The microwave absorption by polymer nanocomposites also depends on polymer to filler mass ratio along with thickness [22]. However, for the present system, percolation threshold was observed. From the table 1, it is observed that the present composite material (PVBMF) has better microwave absorption ability at minimum wt% of filler and thickness as compared to the other MnO_2/Fe based systems.

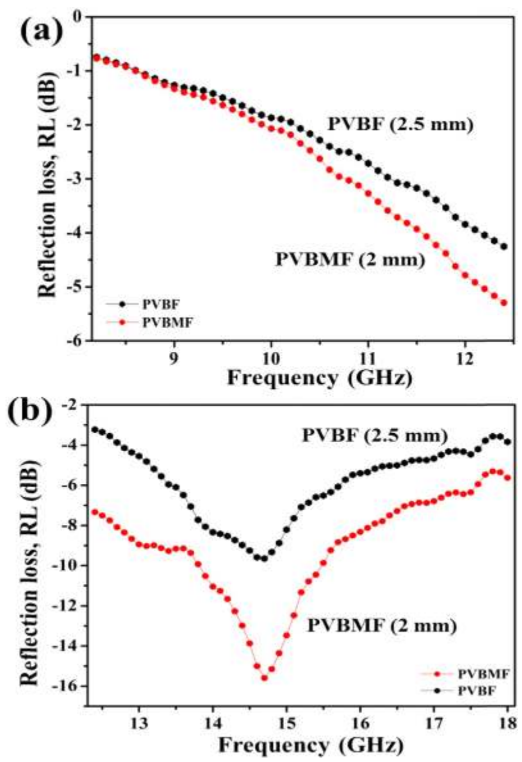

Figure 5. The variation of reflection loss (RL) of PVBMF (thickness 2 mm) and PVBF (thickness 2.5 mm) composites in the (a) X-band (8.2–12.4 GHz) and (b) Ku-band (12.4–18 GHz).

Table 1. Optimum reflection loss (dB) of various reported materials with present work.

Material	Frequency	Reflection loss (dB)	Filler wt%/matrix: filler	Thickness	Reference
Paraffin/Fe granules	~10 GHz	~ −8 dB	40	2 mm	[8]
Paraffin/Fe nanorods	~11.5 GHz	~ −8 dB	40	2 mm	[8]
Paraffin/Fe nanoflakes	~9.5 GHz	~ −10 dB	40	2 mm	[8]
Paraffin/Fe–SiO_2	10 GHz	−14 dB	40	2 mm	[8]
Paraffin/Fe–SiO_2 nanorods	13 GHz	−14 dB	40	2 mm	[8]
Paraffin/MnO_2 micron cube	15.5 GHz	−13.3 dB	30	2 mm	[12]
Paraffin/Fe/C	15 GHz	~ −10 dB	20	1.4 mm	[24]
Epoxy/Fe_2O_3 nanoflowers	10 GHz	−15 dB	80	3 mm	[9]
Epoxy/Fe-CMK3	9.5 GHz	−12 dB	31.8	1.6 mm	[7]
Paraffin/MnO_2–Fe–graphene	12 GHz	−12 dB	1:1	2 mm	[3]
Epoxy/Fe micron fibre	7.5 GHz	−11 dB	20	1.5 mm	[10]
Paraffin/MnO_2 nanorod	5 GHz	−8 dB	1:1	2.5 mm	[3]
Paraffin/MnO_2–Fe nanorod	15 GHz	~ −10 dB	1:1	2.5 mm	[3]
PVB/MnO_2decorated Fe nano cauliflower	14.7 GHz	−15.7 dB	10	2 mm	Present work

For the above system, the input impedance of the system can be written as [21, 23]

$$\eta_{in}(x) = \frac{V(x)}{I(x)} = \eta_0 \frac{\eta_L - j\eta_0 \tan(k.\ x)}{\eta_0 - j\ \tan(k.\ x)} \tag{1}$$

$V(x)$ and $I(x)$ represents the voltage and current at a distance x from the end of the transmission line respectively. η_0, η_L and k corresponds to the intrinsic impedance, load impedance and wave number of the incident electromagnetic wave.

For the present system, $\eta_L = 0$ (As samples were Cu backed).

Therefore, the input impedance of the microwave absorbing material having thickness t_s is given by

$$Z_{in} = -j\ \eta_0 \tan(kt_s) = \eta_0 \tanh(\gamma t_s), \tag{2}$$

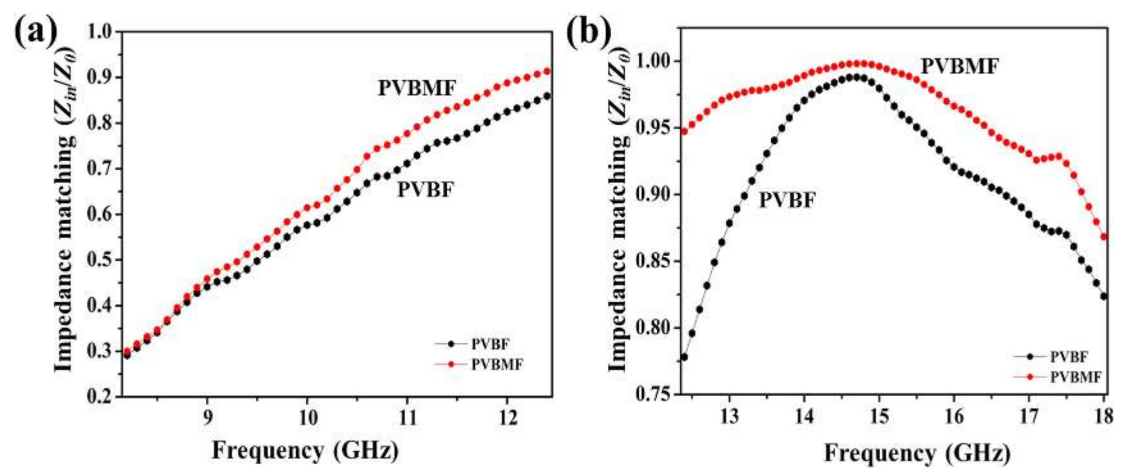

Figure 6. The impedance matching (Z_{in}/Z_o) of PVBMF and PVBF composites in (a) X-band (8.2–12.4 GHz) and (b) Ku-band (12.4–18 GHz).

where, $\gamma = j\omega\sqrt{\eta\varepsilon_r} \; = j2\pi f\sqrt{\eta\varepsilon_r} = j\frac{2\pi}{\lambda_0}\sqrt{\mu_r\varepsilon_r}$ is the propagation constant (ε_r and μ_r are the relative permittivity and permeability of the material, f is the frequency and λ_o is the wavelength of incident electromagnetic wave in air).

The simplified form of equation (2) is

$$Z_{\text{in}} = \eta_0 \tanh\left(j\frac{2\pi t_s}{\lambda_0} \times \sqrt{\mu_r\varepsilon_r}\right) = Z_0\sqrt{\frac{\mu_r}{\varepsilon_r}} \tanh\left(j\frac{2\pi t_s}{\lambda_0} \times \sqrt{\mu_r\varepsilon_r}\right), \tag{3}$$

Thus, the RL of a material is given by following equation

$$\text{RL(dB)} = 20 \log \left|\frac{Z_{\text{in}} - Z_0}{Z_{\text{in}} + Z_0}\right|, \tag{4}$$

where, Z_0 and Z_{in} corresponds to the intrinsic impedance of free space and the composite material respectively.

The impedance matching (Z_{in}/Z_0) of PVBF and PVBMF composite in X-band and Ku- band is shown in the figures 6(a) and (b), respectively. PVBMF composite shows excellent impedance matching as compared to the PVBF composite, in the X-band, the Z_{in}/Z_0 value of PVBMF composite increases linearly from 0.2 to 0.8. Similarly, in the Ku band, the Z_{in}/Z_0 value of PVBMF reached maximum in the 14–15 GHz, the region having minimum RL value. In PVBMF composite, the important factor due to which it shows high impedance matching is the dielectric attenuation. Here, it is associated with the interfacial polarisation, space charge polarisation and relaxation phenomena as it depends on morphology and dispersion of inclusion in the matrix [24]. In other words, these factors are responsible for changing propagation constant of incident microwaves in the PVBMF composite. The real part of the propagation constant (γ) is known as EM attenuation constant (α) which plays the key role in microwave absorption. The EM attenuation constant (α) can be calculated using following equation [25, 26]

$$\alpha = \frac{\sqrt{2}\pi f}{c} \times \left[(\mu''\varepsilon'' - \mu'\varepsilon') + \{(\mu''\varepsilon'' - \mu'\varepsilon')^2 + (\mu'\varepsilon'' + \mu''\varepsilon')^2\}^{\frac{1}{2}}\right]^{\frac{1}{2}}, \tag{5}$$

where c is the velocity of light and f is the frequency of incident electromagnetic wave.

Figures 7(a) and (b) shows the variation of α of PVBF and PVBMF composite in the X and Ku-band respectively. For PVBMF composite, α value increases from 20 to 67 in the X band whilst it was 25–43 for PVBF composite. Similarly, in the Ku band, α value lies 35–59 for PVBF composite which was increased to 67–80 for PVBMF composite. The variation observed in the 14–16 GHz also reveals the maximum absorbing range. Thus, the enhancement of EM attenuation constant of PVMF composite also signifies that the MnO_2 decorated Fe improves the microwave absorption in PVB matrix.

Apart from the above discussions, there is a contribution of scattering attenuation of incident microwave for the obtained RL value of PVBMF composite. The scattering attenuation is a function of the number of nanoparticles in the given volume of the effective medium [22]. The equation of scattering attenuation (I_{sc}) is

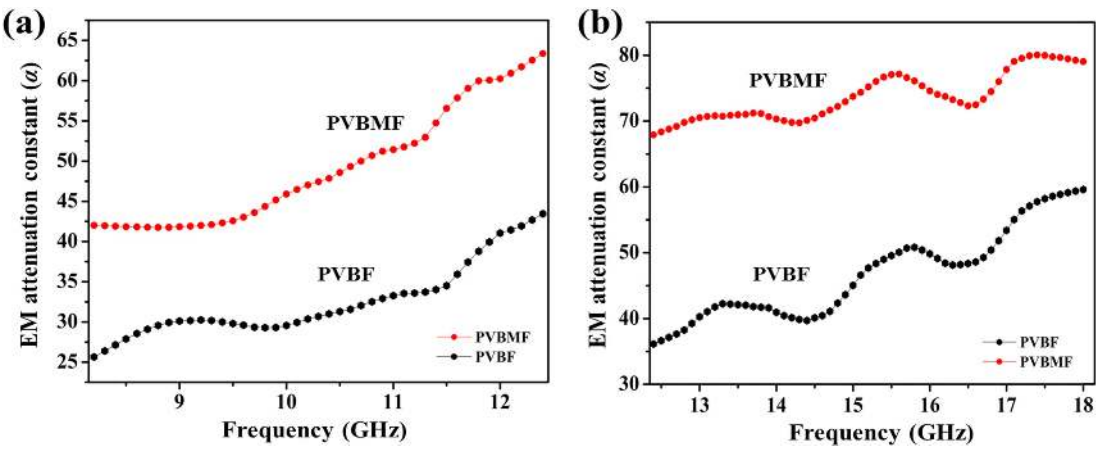

Figure 7. Variation of EM attenuation constant (α) of PVBF and PVBMF composites in the (a) X-band and (b) Ku-band.

$$I_{sc} = I_0 \exp\left\{-n\frac{k^4(|\varepsilon_r - 1|^2 + |\mu_r - 1|^2)}{6\pi}\delta_s\right\}. \tag{6}$$

Here, δ_s is the skin depth of the material.

In PVBMF composite, all the MnO_2–Fe nano cauliflowers are surrounded by effective media. Therefore the incident microwave is also attenuated by scattering and hence microwave absorption increases as the electromagnetic attenuation by a small particle (I_T) is the sum of the absorption attenuation of refracted wave (I_{ab}) and I_{sc} i.e. $I_T = I_{ab} + I_{sc}$ [22]. In case of heterogeneous systems, especially polymer composites, the interfacial polarisation (Maxwell–Wagner–Sillars or MSW effect) is more prominent [27]. For MnO_2 coated Fe nano cauliflowers, the space charge takes place at the interfaces due to the complex permittivity differences between the constituents and it increased significantly in the PVBMF composite as MnO_2–Fe nano cauliflowers were dispersed optimally in the PVB matrix [27]. The inverse of complex permittivity is the complex electric modulus and is associated with dielectric relaxation [27, 28]. Thus, interfacial polarisation (accumulated charge) and associated dielectric relaxation of PVBMF composite also gives a significant RL.

5. Conclusions

The MnO_2 nanofiber decorated Fe (cauliflower morphology) was synthesised by a simple chemical process. MnO_2–Fe nano cauliflower was dispersed in weather resistive PVB matrix and microwave absorption was studied in X-band and Ku-band. The RL of Fe decreased in the presence of MnO_2 and the optimal RL value of -15.7 dB was obtained at 14.7 GHz for 10 wt% loaded PVB/MnO_2–Fe nano cauliflower composite. The factor that strongly enhanced this excellent RL value was found to be impedance matching (Z_{in}/Z_o value reaches maximum in 14.5–15 GHz). Further, enhancement of EM attenuation constant (α), surface morphology, dielectric loss as well as scattering loss also enhances the microwave absorption property of this composite. As PVB based materials are most suitable for coating, the present composite material can also be considered as a coating material to prevent electromagnetic interferences of communication devices as well as for robotic/ microwave engineering.

Acknowledgments

Authors gratefully acknowledge the Department of Science and Technology (SB/S3/ME/51/2012) for financial support. This work is technically supported by IISc advanced characterisation centre and CeNSE. GM thanks the DST for the J C Bose fellowship.

References

[1] Tong X C 2008 *Advanced Materials and Design for Electromagnetic Interference Shielding* (Boca Raton, FL: CRC Press)
[2] Han Z, Li D, Wang H, Liu X G, Li J, Geng D Y and Zhang Z D 2009 Broadband electromagnetic-wave absorption by FeCo/C nanocapsules *Appl. Phys. Lett.* **95** 23114
[3] Lv H, Ji G, Liang X, Zhang H and Du Y 2015 A novel rod-like MnO_2@Fe loading on graphene giving excellent electromagnetic absorption properties *J. Mater. Chem.* C **3** 5056–64

[4] Vinoy K J and Jha R M 2011 Radar absorbing *Materials: From Theory to Design and Characterization* (USA: Springer)
[5] Gooch J W and Daher J K 2007 *Electromagnetic Shielding and Corrosion Protection for Aerospace Vehicles* (New York: Springer)
[6] Saini P, Choudhary V, Vijayan N and Kotnala R K 2012 Improved electromagnetic interference shielding response of poly(aniline)-coated fabrics containing dielectric and magnetic nanoparticles *J. Phys. Chem.* C **116** 13403–12
[7] Wang J, Zhou H, Zhuang J and Liu Q 2015 Magnetic γ-Fe_2O_3, Fe_3O_4, and Fe nanoparticles confined within ordered mesoporous carbons as efficient microwave absorbers *Phys. Chem. Chem. Phys.* **17** 3802–12
[8] Ni X, Zheng Z, Xiao X, Huang L and He L 2010 Silica-coated iron nanoparticles: shape-controlled synthesis, magnetism and microwave absorption properties *Mater. Chem. Phys.* **120** 206–12
[9] Guo C, Xia F, Wang Z, Zhang L, Xi L and Zuo Y 2015 Flowerlike iron oxide nanostructures and their application in microwave absorption *J. Alloys Compd.* **631** 183–91
[10] Wu M, He H, Zhao Z and Yao X 2000 Electromagnetic and microwave absorbing properties of iron fibre-epoxy resin composites *J. Phys. D: Appl. Phys.* **33** 2398
[11] Song W-L *et al* 2014 Nano-scale and micron-scale manganese dioxide vs corresponding paraffin composites for electromagnetic interference shielding and microwave absorption *Mater. Res. Bull.* **51** 277–86
[12] Duan Y, Pang H, Zhang Y, Chen J and Wang T 2016 Morphology-controlled synthesis and microwave absorption properties of β-MnO_2 microncube with rectangular pyramid *Mater. Charact.* **112** 206–12
[13] Duan Y, Liu Z, Jing H, Yin K and Liu S 2013 The effects of annealing treatment on the morphology and microwave absorption properties of α-MnO_2 *Proc. Inst. Mech. Eng.* J **227** 61–9
[14] Saravanan S, Ramamurthy P C and Madras G 2014 Aminosilane functionalized cenosphere in poly(vinyl butyral) composite films: moisture resistant encapsulated Schottky devices *Polym.-Plast. Technol. Eng.* **53** 684–92
[15] Roy A S, Saravanan S, Ramamurthy P C and Madras G 2014 Dielectric impedance studies of poly(vinyl butyral)–cenosphere composite films *Polym. Compos.* **35** 1636–43
[16] Saravanan S, Ramamurthy P C and Madras G 2015 Effects of temperature and clay content on water absorption characteristics of modified MMT clay/cyclic olefin copolymer nanocomposite films: permeability, dynamic mechanical properties and the encapsulated organic device performance *Composites* B **73** 1–9
[17] Meng X and Shen X 2012 Preparation of FeCo-, FeNi- and NiCo-alloy coated cenosphere composites by heterogeneous precipitation *Particuology* **10** 334–8
[18] Chen L F, Ong C K, Neo C P, Varadan V V and Varadan V K 2004 *Microwave Electronics: Measurement and Materials Characterization* (New York: Wiley)
[19] Chu X T A, Ta B N, Ngo L T H, Do M H, Nguyen P X and Nam D N H 2015 Microwave absorption properties of iron nanoparticles prepared by ball-milling *J. Electron. Mater.* **45** 2311–5
[20] Zhuo R F *et al* 2008 Microwave absorption properties and the isotropic antenna mechanism of ZnO nanotrees *J. Appl. Phys.* **104** 94101
[21] Naito Y and Tanaka N 1971 Broad-banding and changing operation frequency of circulator *IEEE Trans. Microw. Theory Tech.* **19** 367–72
[22] Meng H, Song K P, Wang H, Jiang J J, Li D, Han Z and Zhang Z D 2011 Dielectric response of carbon coated TiC nanocubes at 2–18 GHz frequencies *J. Alloys Compd.* **509** 490–3
[23] Guan H, Xie J, Chen G and Wang Y 2014 Facile synthesis of α-MnO_2 nanorods at low temperature and their microwave absorption properties *Mater. Chem. Phys.* **143** 1061–8
[24] Khani O, Shoushtari M Z and Farbod M 2015 Excellent improvement in the static and dynamic magnetic properties of carbon coated iron nanoparticles for microwave absorption *Physica* B **477** 33–9
[25] Zhou M, Zhang X, Wei J, Zhao S, Wang L and Feng B 2011 Morphology-controlled synthesis and novel microwave absorption properties of hollow urchinlike α-MnO_2 nanostructures *J. Phys. Chem.* C **115** 1398–402
[26] Liu X G, Ou Z Q, Geng D Y, Han Z, Xie Z G and Zhang Z D 2009 Enhanced natural resonance and attenuation properties in superparamagnetic graphite-coated FeNi 3 nanocapsules *J. Phys. D: Appl. Phys.* **42** 155004
[27] Tsangaris G M, Psarras G C and Kouloumbi N Electric modulus and interfacial polarization in composite polymeric systems *J. Mater. Sci.* **33** 2027–37
[28] Liu X G, Geng D Y and Zhang Z D 2008 Microwave-absorption properties of FeCo microspheres self-assembled by Al_2O_3-coated FeCo nanocapsules *Appl. Phys. Lett.* **92** 243110